Possible Thermal Decomposition Routes in $[MeB(C_6F_5)_3]^-[L_2TiMe^+]$ as Deactivation Pathways in Olefin Polymerization Catalysis: A Combined Density Functional Theory and Molecular Mechanics Investigation

Tebikie Wondimagegn, Zhitao Xu, Kumar Vanka, and Tom Ziegler*

Department of Chemistry, University of Calgary, Calgary, Alberta, Canada T2N 1N4

Received October 29, 2004

Combined quantum mechanical (QM) and molecular mechanical (MM) models (QM/MM) have been used to explore possible decomposition routes for ion pair systems used as catalysts in olefin polymerization. The catalyst systems include $[MeB(C_6F_5)_3]^-[(NPR_3)_2TiMe^+]$, $[MeB(C_6F_5)_3]^-[(Cp)(NCR_2)TiMe^+]$, and $[MeB(C_6F_5)_3]^-[(Cp)(SiMe_2NR)TiMe^+]$. The possible thermal decomposition routes for the above catalyst systems include fluorine transfer from $[MeB(C_6F_5)_3]^-$ to the metal center, aryl transfer (C_6F_5) to the growing chain, transfer of $B(C_6F_5)_3$ from $[MeB(C_6F_5)_3]^-$ to the ancillary ligand, exchange of methyl on butyl from the ancillary ligand with aryl in $[MeB(C_6F_5)_3]^-$, transfer of hydrogen from the Cp* ring to the growing chain, and transfer of hydrogen from the methyl group on tertiary butyl to the growing chain. The activation barriers fall in the range 15.5−68.7 kcal/mol. The transfer of fluorine from the counterion to the metal center is the most facile deactivation pathway.

Introduction

The development of new single-site olefin polymerization catalysts that do not exclusively contain the bis-cyclopentadienyl (bis-Cp) ancillary ligands has experienced a phenomenal acceleration over the past few years.[1] A variety of strategies have been employed to explore the potential of other ligand systems. The most common way of developing such catalyst systems has been to replace one or both of the Cp ligands in the metallocenes by other donor groups. A notable example of this approach is the so-callled "constrained-geometry catalysts" first introduced by Bercaw[2] in which Cp ligands are combined with an amide functionality. This system is now used commercially by Dow[3] and Exxon.[4] More recently, a number of $Cp(L)TiX_2$ systems (L = OR,[5] NCR_2,[6] NR_2,[7] NPR_3,[8] SR,[9] and alkyl[10]) have been prepared and tested in olefin polymerization catalysis. Stephan et al. have also developed several families of highly active Ti-containing olefin polymerization catalysts with bis(phosphinimide) as ancillary ligands.[11] In general, in conjunction with activators such as methylaluminoxane (MAO), $B(C_6F_5)_3$, and $[A]^+[B(C_6F_5)_4]^-$ (A = CPh_3, HNR_3), the aforementioned complexes have been found to provide catalysts with moderate to high activity, making them viable alternatives to the metallocene systems.

However, these catalyst systems have also been found to undergo deactivating side reactions, leading to the eventual poisoning of the catalyst, thereby decreasing their productivity. The types of deactivation pathways are determined by the strength of the cation−anion interaction. For contact ion pairs, a number of deactivation pathways have been observed for the catalyst systems based on borane and trimethylaluminum activations. The most commonly observed deactivation pathway is C_6F_5-group transfer to the cationic metal center.[12] We have recently reported another commonly observed deactivation pathway, which involves hydrogen transfer from the bridging methyl group to the

* To whom correspondence should be addressed. E-mail: ziegler@ucalgary.ca.

(1) (a) Britovsek, G. P.; Gibson, V. C.; Waas, D. F. *Angew. Chem., Int. Ed.* **1999**, *38*, 429. (b) Liang, L −C.; Schrock, R. R.; Davis, W. M.; McConville, D. H. *J. Am. Chem. Soc*. **1999**, *121*, 5797. (c) Baumann, R.; Stumpf, R.; Davis, W. M.; Liang, l.-C.; Schrock, R. R. *J. Am. Chem. Soc*. **1999**, *121*, 7822. (d) Guerin, F.; Stewart, J. C.; Beddie, C.; Stephan, D. W. *Organometallics* **2000**, *19*, 2994.

(2) (a) Piers, W. E.; Shapiro, P. J.; Bunel, E. E., Bercaw, J. E. *Synlett* **1990**, *1*, 74. (b) Shapiro, P. J.; Cotter, W. D.; Schaefer, W. P.; Labinger, J. A.; Bercaw, J. E. *J. Am. Chem. Soc.* **1994**, *116,* 4623.

(3) Stevens, J. C.; Timmers, F. J.; Wilson, D. R.; Schmidt, G. F.; Nickias, P. N.; Rosen, R. K.; Knight, G. W.; Lai, S. European Patent Appl. EP 416 815-A2, 1991 (Dow Chemical Corp.).

(4) Canich, J. M.; Hlatky, G. G.; Turner, H. W. PCT Appl. WO-A-00333, 1992 (Exxon Chemical Co.).

(5) (a) Vilardo, J. S.; Thorn, M. G.; Fanwick, P. E.; Rothwell, I. P. *Chem. Commun.* **1998**, 2425. (b) Thorn, M. G.; Vilardo, J. S.; Fanwick, P. E.; Rothwell, I. P. *Chem. Commun.* **1998**, 2427. (c) Sarsfield, M. J.; Ewart, S. W.; Tremblay, T. L.; Roszak, A. W.; Baird, M. C. *J. Chem. Soc., Dalton Trans.* **1997**, 3097. (d) Ewart, S. W.; Sarsfield, M. J.; Jeremic, D.; Tremblay, T. L.; Williams, E. F.; Baird, M. C. *Organometallics* **1998**, *17*, 1502.

(6) Zhang, S.; Piers, W. E.; Gao, X.; Parvez, M. *J. Am. Chem. Soc*. **2000**, *122,* 5499.

(7) (a) Bai, Y.; Roesky, H. W.; Noltmeyer, M. *Z. Anorg. Allg. Chem.* **1991**, *31*, 3887. (b) Schiffino, R. S.; Crowther, D. J. U.S. patent No. 5,625,016, 1997 (Exxon Chemical Co.).

(8) Stephan, D. W.; Stewart, J. C.; Guerin, F.; Spence, R. E. v. H.; Xu, W.; Harrison, D. G. *Organometallics* **1999**, *18*, 1116.

(9) Klapötke, T.; Laskowski, R.; Köpf, H. *Z. Naturforsch., Teil B* **1987**, *42*, 777.

(10) (a) Ewart, S. W.; Baird, M. C. *Top. Catal.* **1999**, *7*, 1. (b) Mena, M.; Royo, P.; Serrano, R.; Pellinghelli, A.; Tiripicchio, A. *Organometallics* **1989**, *8*, 476.

(11) Stephan, D. W.; Guerin, F.; Spence, R. E. v. H.; Koch, L.; Gao, X.; Brown, S. J.; Swabey, J. W.; Wang, Q.; Xu, W.; Zoricak, P.; Harrison, D. J. *Organometallics* **1999**, *18*, 2046.

(12) Wondimagegn, T.; Xu, Z.; Vanka, K.; Ziegler, T. *Organometallics* **2004**, *23*, 3847.

10.1021/om049157g CCC: $30.25
Publication on Web 03/23/2005

Scheme 1. Hydride Transfer Decomposition Pathways Involving the Ketimide Catalyst[a]

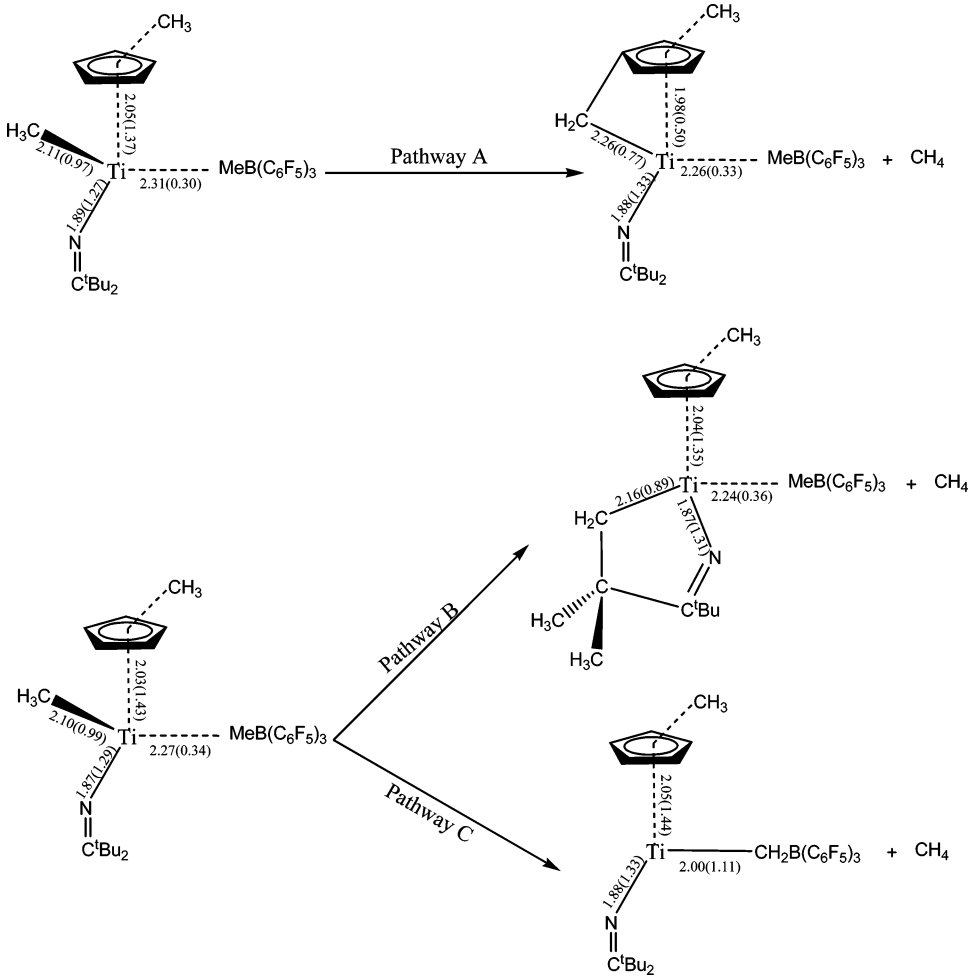

[a] Selected bond distances (Å) and bond orders (in parentheses) are shown for reactants (left) and products (right).

growing chain.[13] In this study, we report additional competing thermal deactivation pathways involving the ion pair $[MeB(C_6F_5)_3]^-[L_2TiMe^+]$.

Computational Methods and Details

Density functional theory calculations were carried out using the Amsterdam Density Functional (ADF) program system, developed by Baerends et al.[14] and vectorized by Ravenek.[15] The numerical integration scheme applied was developed by te Velde et al.,[16] and the geometry optimization procedure was based on the method of Verslius and Ziegler.[17]

Slater-type double-ζ plus polarization basis sets were employed for H, B, C, N, O, F, Si, P, and Cl atoms, while a triple-ζ plus polarization basis set was used for the Ti atom. All calculations were based on the PW91 exchange−correlation functional.[18] Combined quantum mechanical (QM) and molecular mechanical (MM) models (QM/MM) have been applied throughout this study. In this model, QM/MM atoms were employed to model the tertiary butyl groups, with hydrogens used as capping atoms. For systems involving the tertiary butyl group itself, QM atoms have been employed. The MM atoms were described using the SYBYL/TRIPOS 5.2 force field constants.[19] The code for QM/MM in ADF has been implemented by Woo et al.[20] The QM/MM model for $[MeB(C_6F_5)_3]^-$ has been validated in a previous study.[21]

Results and Discussion

In this paper, we report the results from theoretical investigations on thermal decomposition routes involving the ion pair systems. We shall demonstrate how electronic and steric effects can modify the activation barrier.

A. Intramolecular C−H Activation. Scheme 1 displays three possible deactivation pathways based on intramolecular C−H activation. Pathway A represents transfer of hydrogen from C_5Me_5 (Cp*) to the growing polymer (CH_3), whereas pathway B involves the transfer

(13) Wondimagegn, T.; Vanka, K.; Xu, Z.; Ziegler, T. *Organometallics* **2004**, *23*, 2651.

(14) (a) Baerends, E. J.; Ellis, D. E.; Ros, P. *Chem. Phys.* **1973**, *2*, 41. (b) Baerends, E. J.; Ros, P. *Chem. Phys*. **1973**, *2*, 52. (c) te Velde, G.; Baerends, E. J. *J. Comput. Phys*. **1992**, *92*, 84. (d) Fonseca, C. G.; Visser, O.; Snijders, J. G.; te Velde, G.; Baerends, E. J. In *Methods and Techniques in Computational Chemistry, METECC-95*; Clementi, E., Corongiu, G., Eds.; STEF: Cagliari, Italy, 1995; p 305.

(15) Ravenek, W. In *Algorithms and Applications on Vector and Parallel Computers*; te Riele, H. J. J., Dekker: T. J., vand de Horst, H. A., Eds.; Elservier: Amsterdam, 1987.

(16) (a) te Velde, G.; Baerends, E. J. *J. Comput. Chem.* **1992**, *99, 84*. (b) Boerrigter, P. M.; te Velde, G.; Baerends, E. J. *Int. J. Quantum Chem.* **1998**, *33,* 87.

(17) Verslius, L.; Ziegler, T. *J. Chem. Phys*. **1988**, *88,* 322.

(18) Perdew, J. P.; Chevary, J. A.; Vosko, S. H.; Jackson, K. A.; Pederson, M. R.; Fiolhais, C. *Phys. Rev. B* **1992**, *46*, 6671.

(19) Clark, M.; Cramer, R. D. I.; van Opdenbosch, N. *J. Comput. Chem*. **1989**, *10*, 982.

(20) Woo. T. K.; Cavallo, L.; Ziegler, T. *Theor. Chim. Acta* **1998**, *100*, 307.

(21) Xu, Z.; Vanka, K.; Firman, T.; Michalak, A.; Zurek, E.; Zhu, C.; Ziegler, T. *Organometallics* **2002**, *21*, 2444.

Table 1. Activation Energies and Heat of Reaction (kcal/mol) for Hydrogen Transfer[a]

pathway	heat of reaction	activation energy
A	11.0	38.3
B	15.5	34.0
C	7.1	21.9

[a] The catalyst is (Cp)(NCR_2)TiMe-μ-MeB(C_6F_5)$_3$ in all cases.

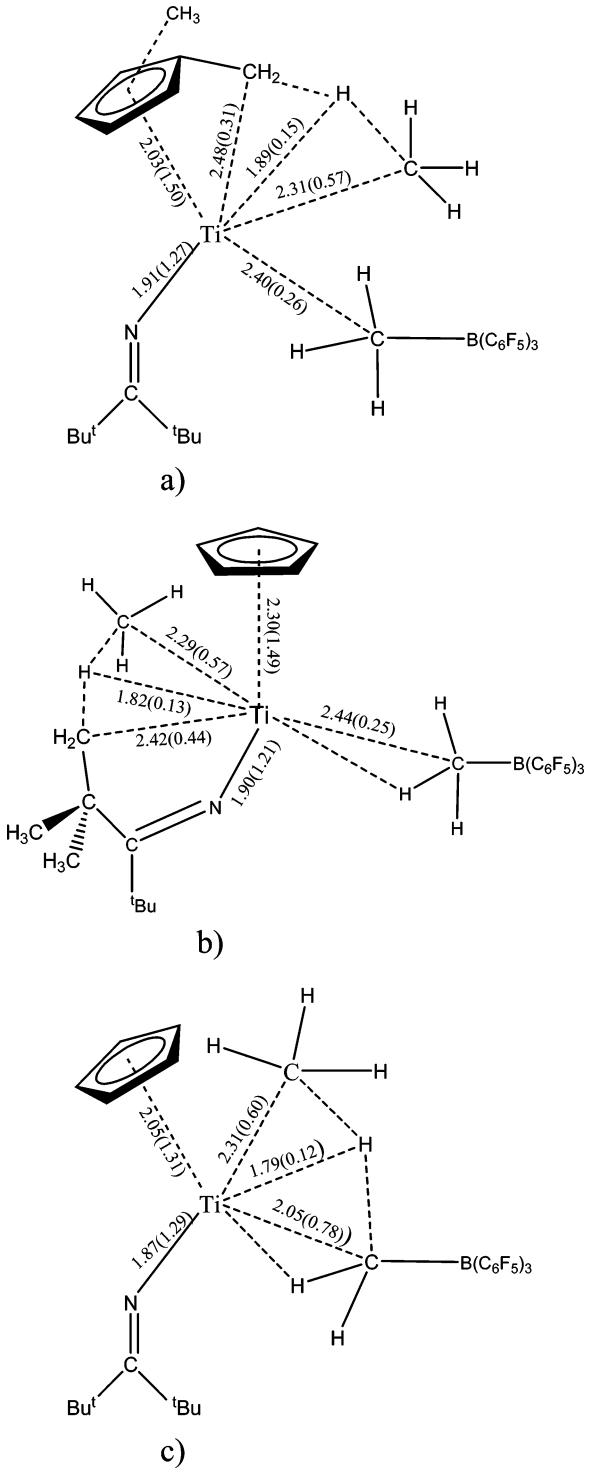

Figure 1. Selected optimized transition state geometries (Å) and bond orders (in parentheses) for hydride transfer reactions involving pathways A (a), B (b), and C (c).

of hydrogen from the ancillary ligand to methyl attached to the metal center. Finally, pathway C depicts the transfer of hydrogen from the counterion to the growing polymer. All these reactions produce methane. Pathway C has been studied both experimentally[6] and theoretically[13] for the ketimide catalyst [MeB(C_6F_5)$_3$]$^-$[(Cp)(NCR_2)TiMe]$^+$. We shall for comparison restrict our study of pathways A and B to the same system.

Table 2. Activation Energies and Heat of Reaction (kcal/mol) for the Fluoride Transfer Process

catalyst	heat of reaction	activation energy
(NPR_3)$_2$TiMe-μ-MeB(C_6F_5)$_3$	−39.5	24.8
($CpSiMe_2NR$)TiMe-μ-MeB(C_6F_5)$_3$	−57.8	15.5

Table 1 presents the activation energies and heat of reaction for all three hydrogen transfer reactions. As illustrated in the table, the activation barriers fall in the range 22−38 kcal/mol. The lowest activation barrier was obtained for the transfer of hydrogen from the counterion to the growing polymer (pathway C). This reaction pathway has been extensively studied for a variety of catalyst systems in our laboratory.[13] Pathways A and B have also been studied for the cationic catalyst L_2TiMe^+.[22]

Figure 1 depicts optimized transition state geometries and bond orders for all three hydrogen transfer reactions. As can be seen from the figure, the reaction involves the breakage of two bonds, the C−H and Ti−CH_3 linkages, and the corresponding formation of two bonds, Ti−CH_2R and H−CH_3. For the hydrogen transfer reaction to take place, for pathways A, B, and C, the methyl group on the Cp* ring, the methyl group on butyl, and the bridging methyl group in MeB(C_6F_5)$_3^-$ have to lose a hydrogen to the accepting α-carbon in the growing polymer (CH_3), respectively. It is thus clear that the interaction between the metal center and the CH_2R carbon (the carbon that has undergone C−H activation) is an important factor for determining the activation barrier for A, B, and C.

In pathway C, the carbon undergoing C−H activation is already coordinated to the metal center as part of the anion in the reactant, whereas the C−H activated carbons in A and B have to establish Ti−C bonds by increasing the coordination around the metal; see Scheme 1 and Figure 1. The Ti−CH_2R distances in the transition states of A and B at 2.48 and 2.42 Å, respectively, are as a consequence longer than for C at 2.05 Å and the barriers for A and B are correspondingly higher (see Figure 1 and Table 1). We also note that the activated hydrogen on route to the CH_3 growing chain in the transition states are stabilized by Ti−H interactions. The Ti−H distance is shortest for C, Figure 1, with the least coordinated metal center. This again helps to stabilize the TS of C compared to A and B. In general, the barriers for the three pathways correlate well with the Ti−CH_2R and Ti−H distances, Figure 1, with the order A > B > C.

Our analyses here of the barriers for A, B, and C were also supported by a bond order[23] analysis, which clearly finds C to have the largest bond order for the Ti−H and Ti−CH_2R linkages, Figure 1. For the heat of reaction,

(22) Wondimagegn, T.; Xu, Z.; Vanka, K.; Ziegler, T. *Organometallics* **2004**, *23*, 5737−5743.

(23) Michalak, A.; DeKock, R. L.; Ziegler, T. Manuscript in preparation. The bond order method employed in this work is a modification of that published by Nalewajski and co-workers. (a) Nalewajski, R. F.; Mrozek, J. *Int. J. Quantum Chem.* **1994**, *51*, 187. (b) Nalewajski, R. F.; Mrozek, J.; Michalak, A. *Int. J. Quantum Chem.* **1997**, *61*, 589.

Scheme 2. Fluoride Transfer Reactions

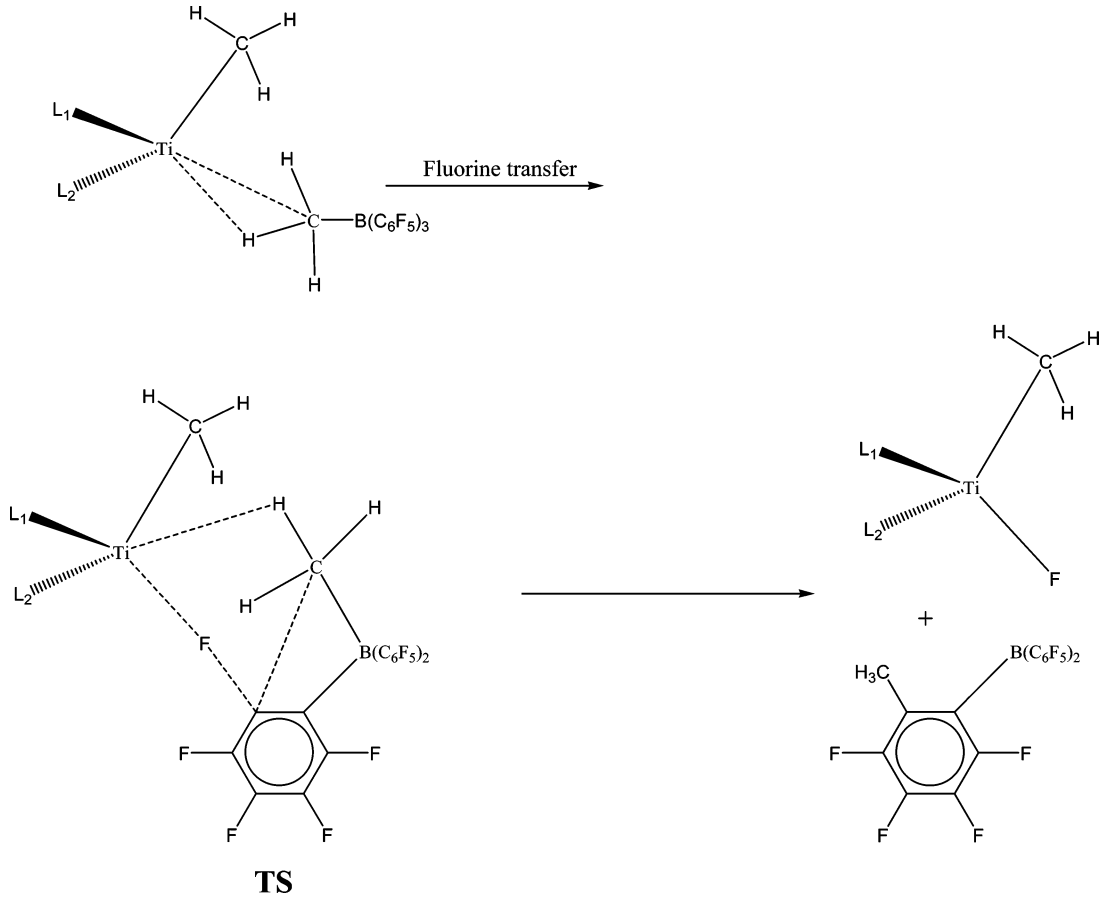

pathway C is again most favorable. However, the order for the other two pathways has now been changed to B > A. Our bond order analysis, Scheme 1, of the products indicates that the Ti−Cp* bond order increases in A but not in B after C−H activation.

Pathway A is a commonly observed deactivation reaction. Marks et al. have reported the reaction of the bulky precatalyst $(1,3\text{-}^{t}Bu_2Cp)_2ZrMe_2$ with the activator $B(C_6F_5)_3$ to produce a C−H-activated metallacyclic cation.[24] The product formed in this reaction is inactive with respect to ethylene polymerization or oligomerization. Marks et al. have also studied the reaction of Cp^*TiMe_3 with $B(C_6F_5)_3$ to form an intramolecularly metalated fulvene-type cationic complex and methane.[25] Such a complex has been observed previously in the case of a dibenzyl precursor of the constrained-geometry catalyst.[26] Erker et al. have investigated the reaction of the precatalyst $(C_4H_5CMe_2NMe_2)_2Zr(CH_3)_2$ with the activator $B(C_6F_5)_3$.[27] The resulting methylzirconocene cation is extremely reactive with regard to an intramolecular C−H activation reaction. The observed C−H activation process takes place at the N−CH_3 group, involving a four-centered transition state.

B. Fluorine Transfer to the Metal. Table 2 displays activation energies and heat of reaction for the fluoride transfer pathway shown in Scheme 2. It follows from Table 2 that these reactions are highly exothermic and the activation energies are 15.5 and 24.8 kcal/mol for CGC and the bis(phosphinimide) systems, respectively. This is the most facile ion pair deactivation pathway we have encountered so far.

As illustrated in Scheme 2, the fluorine transfer reaction forms a four-centered transition state. The fluorine leaves the aryl group as F^-, forming a positive charge on the ring. In a similar way, the bridging methyl group in $CH_3B(C_6F_5)_3^-$ leaves as CH_3^-, making the metal center more positive. We have carried out a bond order analysis to evaluate the total bonding around titanium. The bis(phosphinimide) catalyst has a higher bond order (4.46) around titanium than the constrained-geometry catalyst (4.15) system. It is thus clear that CGC is more susceptible (electropositive) for further coordination than the bis(phsophinimide) system. In the transition state, the metal center in CGC can more readily accept the incoming F^-. This is reflected by the lower barrier reported for this system.

The optimized transition state structures for the fluoride transfer reactions are shown in Figure 2. As seen from the figure, the Ti−F distances are 1.95 and 2.01 Å for the constrained-geometry and the bis(phosphinimide) catalyst systems, respectively. For the constrained-geometry catalyst, the F−C_6F_5, CH_3−C_6F_5, and CH_3−B distances are 1.60, 2.16, and 1.96 Å, respectively. The corresponding distances for bis(phsphinimide catalyst systems are 1.51, 3.1, and 1.61 Å, respectively.

(24) (a) Yang, X.; Stern, C. L.; Maks, T. J. *J. Am. Chem. Soc*. **1994**, *116*, 10015. (b) Yang, X.; Stern, C. L.; Maks, T. J. *J. Am. Chem. Soc*. **1991**, *113*, 3623.

(25) Chen, Y.-X.; Metz, M. V.; Li. L.; Stern, C. L.; Marks, T. J. *J. Am. Chem. Soc*. **1998**, *120*, 6287.

(26) Chen, Y.-X.; Marks, T. J. *Organometallics* **1997**, *16*, 3649.

(27) Bertuleit, A.; Fritze, C.; Erker, G.; Frohlich, R. *Organometallics* **1997**, *16*, 2891.

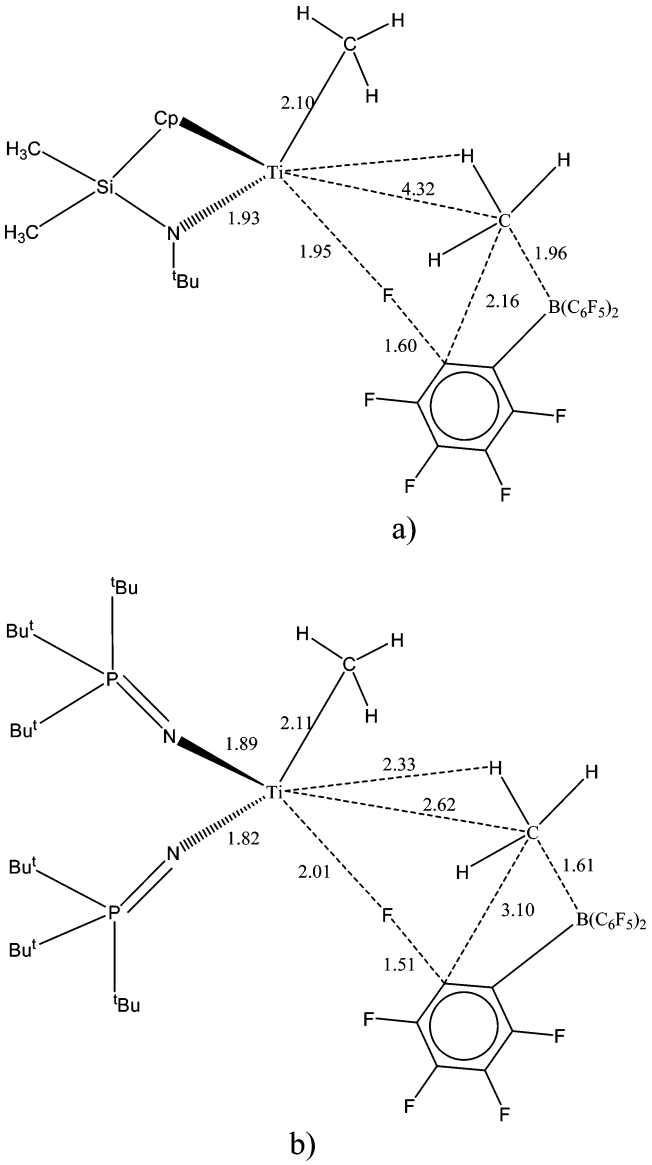

Figure 2. Optimized transition state geometries (Å) for fluoride transfer reactions involving the constrained-geometry (a) and the bis(phosphinimide) (b) catalyst systems.

All the structural parameters presented above corroborate the observed activation barrier differences between these systems. For example, the Ti−F distance in CGC is shorter than the corresponding distance in bis(phosphinimide) systems. Thus, the interaction between the metal center and the fluorine atom is stronger in the constrained-geometry catalyst system. This appears to be the case that stabilizes the transition state, as evidenced by the lower barrier reported for the CGC system.

This deactivation pathway has been investigated experimentally by Marks et al.[22a] Prolonged standing of a solution of $Cp^*ZrCH_3^+B(C_6F_5)_3CH_3^-$ in benzene at 25 °C results in the formation of the fluoride-bridged complex $[Cp^*_2(CH_3)Zr(\mu\text{-}F)Zr(CH_3)\text{-}Cp^*_2]^+CH_3B(C_6F_5)_3$. This complex can be viewed as an adduct between $Cp^*ZrCH_3^+B(C_6F_5)_3CH_3^-$ and $Cp^*_2Zr(CH_3)F$. Marks et al. have proposed two possible mechanisms for the formation $Cp^*_2Zr(CH_3)F$. The first mechanism involves the transfer of an aryl group to the metal center to form $Cp^*_2ZrCH_3C_6F_5$ and $CH_3B(C_6F_5)_2$, followed by *o*-fluoride abstraction to form $Cp^*_2Zr(CH_3)F$ and organoboron species. The second mechanism involves direct fluoride transfer to the zirconium cation. We have considered the latter mechanism for our theoretical investigation and found that it indeed is a plausible deactivation pathway.

Table 3. Activation Energies and Heat of Reaction (kcal/mol) for Aryl Group Transfer

catalyst	heat of reaction	activation energy
$(NPR_3)_2TiMe\text{-}\mu\text{-}MeB(C_6F_5)_3$	13.6[a]	38.5
$(CpSiMe_2NR)TiMe\text{-}\mu\text{-}MeB(C_6F_5)_3$	3.0[b] (32.6)[c]	35.9

[a] Product (c) of Figure 4. [b] Product (b) of Figure 4. [c] Product (a) of Figure 4.

C. Aryl Transfer to the Growing Chain. The activation energies and heat of reaction for the aryl group transfer reaction from the counterion to the growing chain are shown in Table 3. This reaction is presented in Scheme 3. The aryl group transfer reactions are endothermic, and the activation energies are 35.9 and 38.5 kcal/mol for the constrained-geometry catalyst and bis(phsophinimide) systems, respectively. This reaction is also a possible deactivation pathway and may compete with ring-metalated intramolecular C−H activation reactions discussed above. The CGC catalyst has a lower activation barrier than the bis(phophinimide) system. The optimized transition state structures depicted in Figure 3 do not show the observed differences in activation energy between the two systems. The lower barrier obtained for the CGC system is due to steric effects. The steric bulk of the bis(phosphinimide) ligand is larger than the CGC system. Attempts to optimize the product formed from the aryl group transfer reaction as shown in Scheme 3 failed for the bis(phsophinimide) system. Instead, we obtained a four-coordinated product, presented in Figure 4. The unexpected product observed for the bis(phosphinimide) catalyst system prompted us to undertake similar calculation for the CGC catalyst. It indeed gave a product that is more stable than the complex outlined in Scheme 3. The new bonds, Ti−H and $Ti-CH_2B(C_6F_5)_2$, stabilize the product complex. The $Ti-CH_3$ (bridging methyl) bond in CGC is considerably displaced from the metal center, and there are no new bonds formed (see Figure 4). As discussed in the previous section, the CGC catalyst system is more susceptible for further coordination than the bis(phosphinimide) system. This explains why the CGC system (final product in Figure 4b) is more thermodynamically favorable than the bis(phosphinimide) system (only product formed in Figure 4c).

D. Exchange of Methyl on Butyl with Aryl in $B(C_6F_5)_3$. Scheme 4 exhibits exchange of methyl on butyl with aryl in $B(C_6F_5)_3$. The activation energies and the heat of reactions are given in Table 4. The activation barriers are high, and thus, this deactivation pathway is not a likely decomposition route for these catalyst systems. As can be seen from the scheme, the reaction involves the breakage of two strong bonds, $C-CH_3$ and $B-C_6F_5$, and the corresponding formation of two new bonds, $C-C_6F_5$ and $B-CH_3$. The transition state structures reveal that the $B-C_6F_5$ bond has lengthened considerably. At the same time, there has only been a

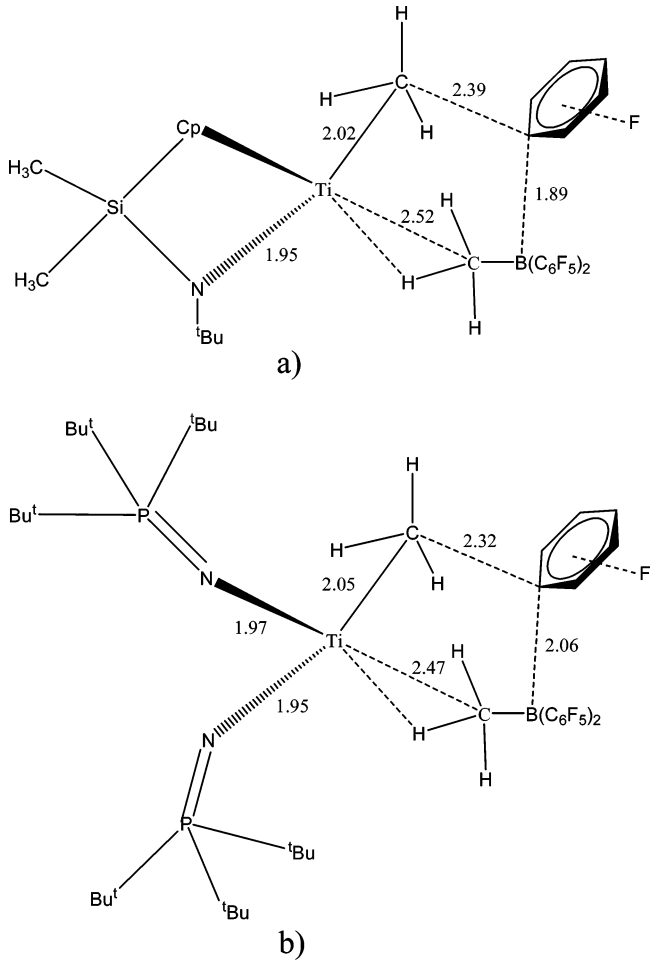

Figure 3. Optimized transition state geometries (Å) for the aryl group transfer reactions involving the constrained-geometry (a) and the bis(phosphinimide) (b) catalyst systems.

Scheme 3. Aryl Group Transfer to the Growing Polymer

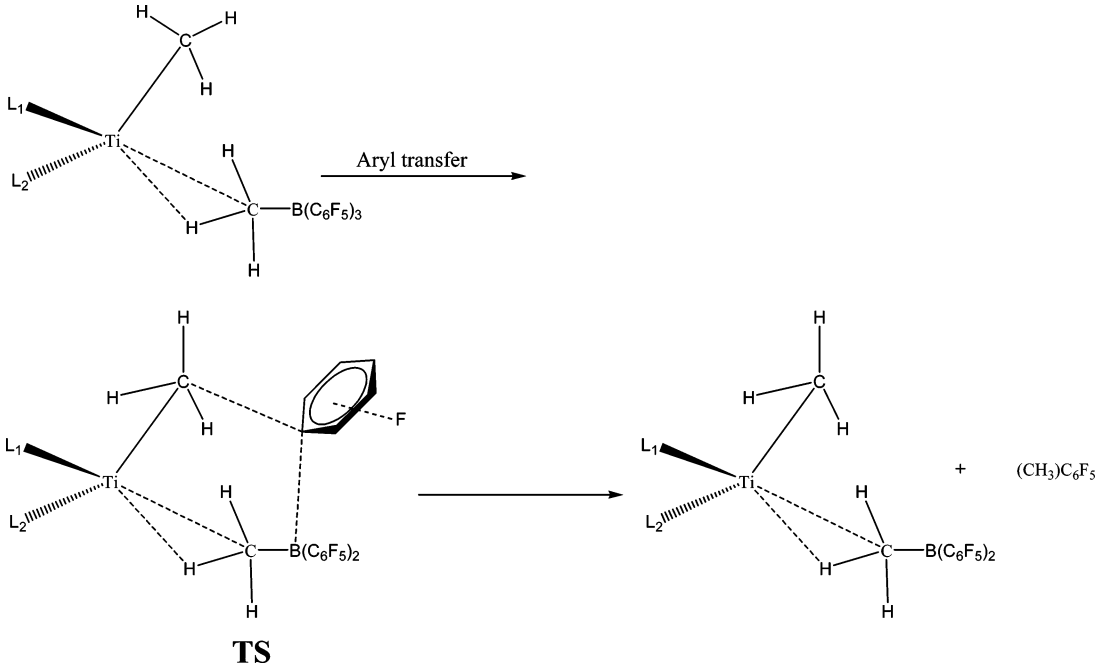

partial formation of the $C-C_6F_5$ bond, while the formation of the $B-CH_3$ bond has not occurred (see Figure 5). This explains the very high barriers observed for this reaction.

E. $B(C_6F_5)_3$ Group Transfer to Nitrogen of the Ancillary Ligand. Table 5 shows the heats of reaction for $B(C_6F_5)_3$ transfer to nitrogen of the ancillary ligand for CGC and bis(phosphinimide) systems. As shown in

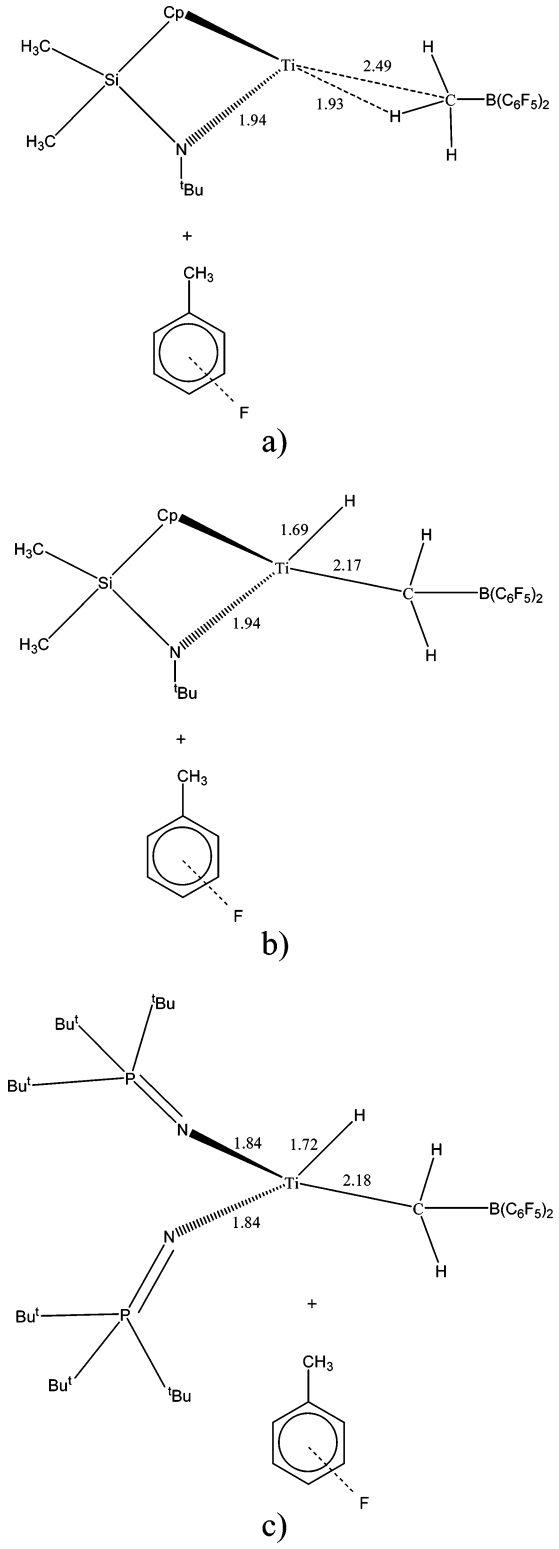

Figure 4. Selected optimized geometries (Å) of products formed from the decomposition involving aryl transfer to the growing chain. (a) Initial product formed by constrained-geometry catalyst. (b) Final product formed by constrained-geometry catalyst after hydride transfer to the metal. (c) Only product formed by bis(phosphinimide).

Scheme 5, this involves the breakage of a strong bond, $B-CH_3$, and the corresponding formation of a new bond, B−N. The $B-CH_3$ bond is stronger than the B−N bond; that is why this deactivation pathway is thermodynamically unfavorable.

F. Aryl Group Transfer to Metal and $CH_3B(C_6F_5)_2$ Transfer to Nitrogen of the Ancillary Ligand. Also, Table 5 presents the heats of reaction for aryl transfer to the metal center and $CH_3B(C_6F_5)_2$ group transfer to the nitrogen of the ancillary ligand. This deactivation pathway is highly endothermic for both compounds, and we have not attempted to locate the transition states for the above systems. As outlined in Scheme 6, the $Ti-CH_3$ (bridging methyl) and $B-C_6F_5$ bonds are broken, whereas the B−N and $Ti-C_6F_5$ bonds are formed in the course of the reaction. The $B-C_6F_5$ bond is stronger than the B−N bond. Thus, from a thermodynamic point of view, this deactivation pathway is not a likely decomposition route for these catalyst systems.

G. Crossover Temperatures. Industrial-scale olefin polymerization processes are usually performed at high temperatures with a minimum pressure of 5 bar. In gas-phase processes, the temperatures are kept in the range from 80 to 100 °C, whereas the solution processes require temperatures above 100 °C. The kinetics and deactivation of single-site olefin polymerization catalysts at higher temperatures and pressure are therefore of great interest for industrial-scale applications. It is therefore important to compare rates of decomposition k_d and rates of propagation k_p. It is reasonable to consider that the catalyst deactivates at a certain temperature T_x when the observed propagation rate k_p^{obs} is equal to the rate of decomposition k_d. We shall refer to T_x as the crossover temperature. It should be noted that $k_p^{obs} = k_p[M]$, where [M] is the concentration of monomer. Both rate constants at standard conditions can be expressed by using the Eyring equation, as shown below, where k_B is the Boltzmann constant and h is Planck's constant.

$$\ln\left(\frac{k_c}{T}\right) = \left(\frac{-\Delta H^{\ddagger}_c}{RT}\right) + \left(\frac{\Delta S^{\ddagger}_c}{R}\right) + \ln\left(\frac{K_B}{h}\right); c = d, p \quad (1)$$

Here $\Delta H^{\ddagger}_p$ and $\Delta H^{\ddagger}_d$ are the enthalpy of activation for the propagation and deactivation step, respectively, whereas $\Delta S^{\ddagger}_p$ and $\Delta S^{\ddagger}_d$ are the corresponding entropies. We obtain by equating k_p^{obs} *and* k_d and solving for T_x that

$$T_x = \frac{\Delta H^{\ddagger}_p - \Delta H^{\ddagger}_d}{\Delta S^{\ddagger}_p - \Delta S^{\ddagger}_d + R\ln([M])} \quad (2)$$

The concentration term in eq 2 can be replaced with partial pressure because we are dealing with gas-phase reactions. It should be noted that the propagation process in general must have a lower barrier than the decomposition process ($\Delta H^{\ddagger}_p < \Delta H^{\ddagger}_d$) for the catalyst to be active at any temperature. Also, the propagation step is bimolecular, whereas the decomposition process under investigation is unimolecular; thus $\Delta S^{\ddagger}_d > \Delta S^{\ddagger}_p$. Under these conditions, one is assured to obtain a physically meaningful positive value for T_x. However, for bimolecular reactions one would obtain either a rather high T_x ($\Delta S^{\ddagger}_d \approx \Delta S^{\ddagger}_p$) or no crossover at all ($\Delta S^{\ddagger}_d < \Delta S^{\ddagger}_p$). Thus bimolecular decomposition reactions are not likely candidates for deactivation as unimolecular decomposition reactions.

Scheme 4. Exchange of Methyl on *tert*-Butyl with Aryl Group in $B(C_6F_5)_3$[a]

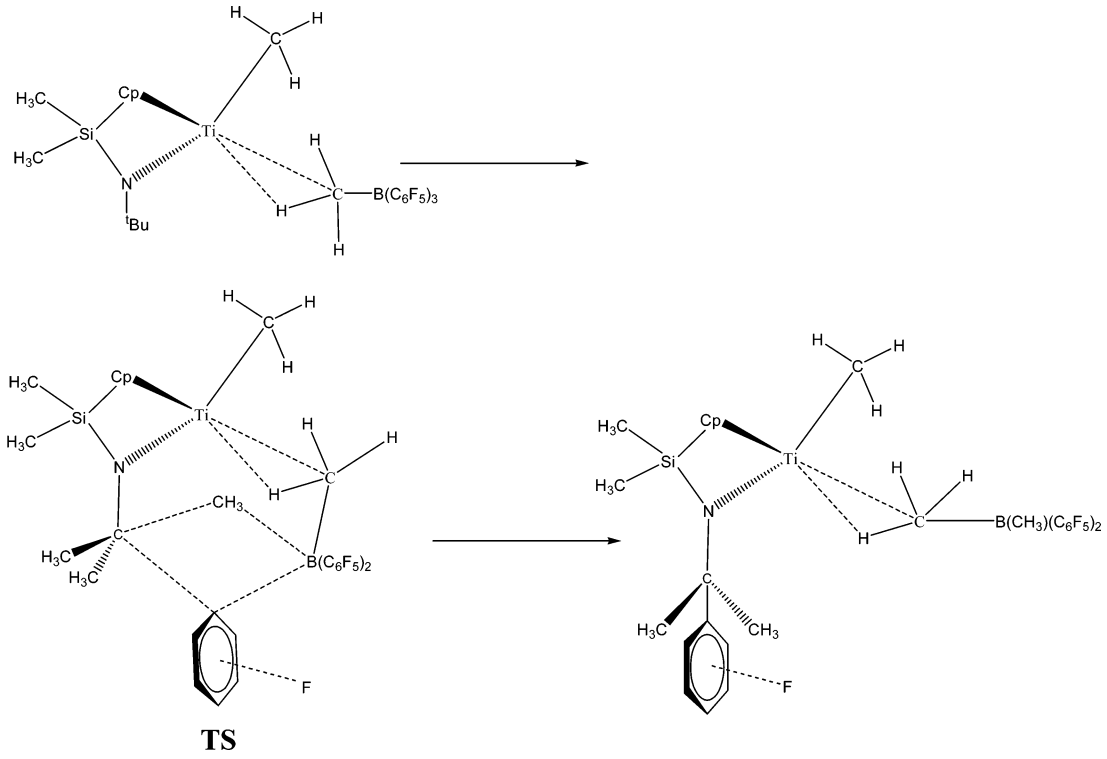

[a] This scheme is also applicable for bis(phsophinimide) system.

Scheme 5. $B(C_6F_5)_3$ Group Transfer to Nitrogen of the Ancillary Ligand

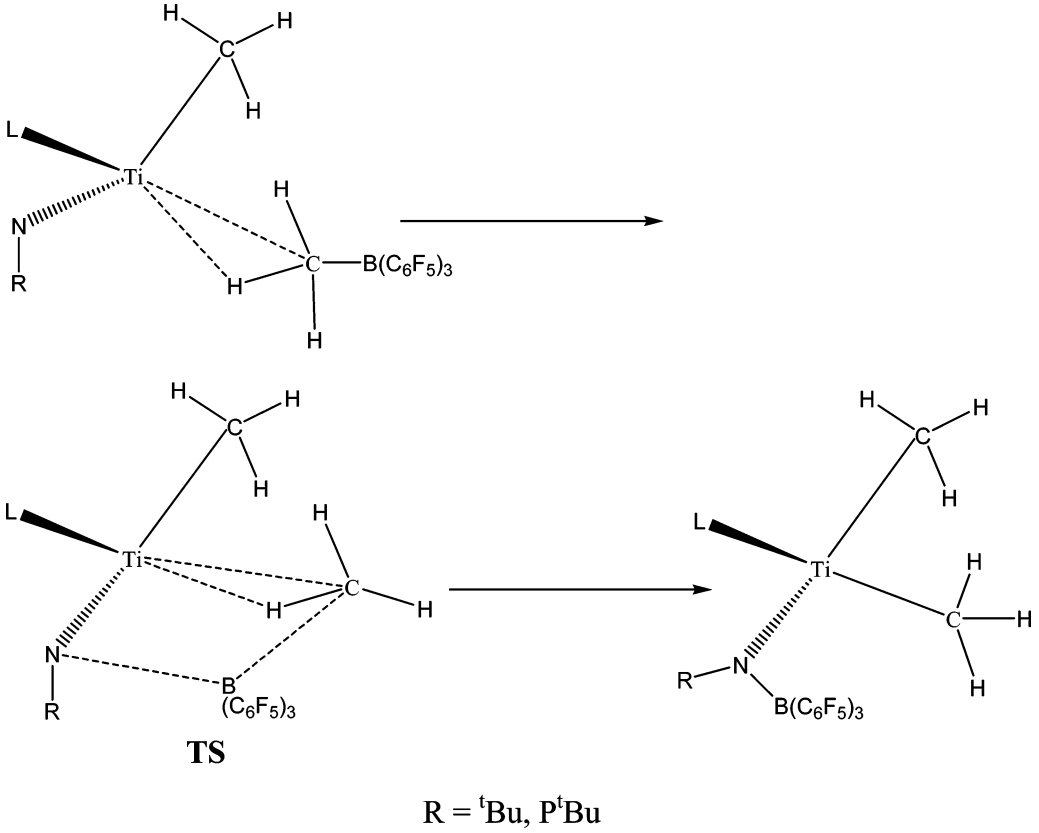

R = ^{t}Bu, P^{t}Bu

It is difficult to obtain an accurate experimental[28] or theoretical[29] estimate for the enthalpic and entropic parameters entering eq 2. We shall in the following adopt a common average value of $\Delta H^{\ddagger}_p = 12.0$ kcal/mol for the barrier to insertion of ethylene into the Ti−Me bond, in close agreement with the few available experimental[28] and theoretical[29] data. The barrier of decom-

(28) Liu, Z.; Somsook, E.; White, C. B.; Rosaaen, K. A.; Landis, C. R. *J. Am. Chem. Soc*. **2001**, *123,* 11193.

(29) Vanka, K.; Xu, Z.; Ziegler, T. *Isr. J. Chem.* **2002**, *42*, 403.

Table 4. Activation Energies and Heat of Reaction (kcal/mol) for Exchange of Methyl on Butyl with Aryl Group in $B(C_6F_5)_3$

catalyst	heat of reaction	activation energy
$(NPR_3)_2TiMe$-μ-$MeB(C_6F_5)_3$	16.6	68.7
$(CpSiMe_2NR)TiMe$-μ-$MeB(C_6F_5)_3$	10.7	62.4

position ($\Delta H^{\ddagger}_d$) will on the other hand be taken from the calculated values in Tables 1−5.

Most problematic are the activation entropies. It is possible (but costly) to calculate theoretical $\Delta S^{\ddagger}$ values. Further, these values correspond to the gas phase, and it is not easy to calculate the corresponding activation entropies in solution. We adopt for $\Delta S^{\ddagger}_p$ a value of −33 cal/mol K typical for a bimolecular insertion reaction.[28] The monomolecular decomposition reaction can be expected to have $\Delta S^{\ddagger}_d \approx 0.0$ cal/mol K. For $[Cp(^tBu_2C{=}N)TiMe]^+[MeB(C_6F_5)_3]^-$, the observed[6] $\Delta S^{\ddagger}_d$ value is −8.5 cal/mol K, whereas we have obtained a theoretical gas-phase value of −2.7 cal/mol K. We will make use of all three values for the various decomposition pathways in order to gauge how a spread (uncertainty) of ∼9 cal/mol K influences the estimated T_x values.

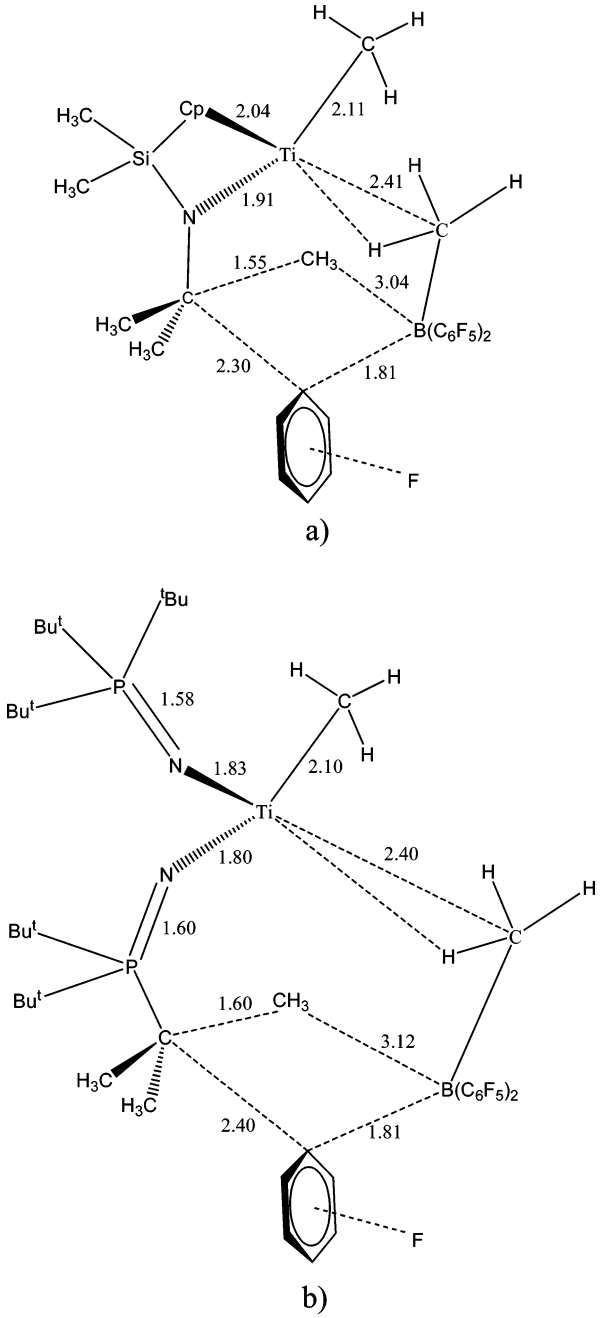

Figure 5. Optimized transition state geometries (Å) for the exchange of aryl in $B(C_6F_5)_3$ and methyl on *tert*-butyl. This involves the constrained-geometry (a) and the bis-(phosphinimide) (b) catalyst systems.

Table 5. Heat of Reaction (kcal/mol) for $B(C_6F_5)_3$ and $CH_3B(C_6F_5)_2$ Transfer Reactions

catalyst	heat of reaction	
$(NPR_3)_2TiMe$-μ-$MeB(C_6F_5)_3$	59.4[a]	32.6[b]
$(CpSiMe_2NR)TiMe$-μ-$MeB(C_6F_5)_3$	46.7[a]	43.2[b]

[a] Heat of reaction for $B(C_6F_5)_3$ transfer to nitrogen of the ancillary ligand; see Scheme 5. [b] Heat of reaction for $CH_3B(C_6F_5)_2$ transfer to L and aryl group transfer to the metal; see Scheme 5.

Table 6 presents the crossover temperature at different entropies of activation. Here we shall illustrate the utility of simulated crossover temperatures (Table 6) for comparing the activity of the catalysts at higher temperatures (100−250 °C). For hydrogen transfer reactions, the crossover temperatures ($\Delta S^{\ddagger}_d = 0$ cal/mol K) are 797, 667, and 300 K for pathways A, B, and C, respectively. Thus, pathways A and B would not occur at 100 and 250 °C. However, pathway C would occur at 100 °C. If $\Delta S^{\ddagger}_d = -2.7$ cal/mol K (calculated value), we would get a different picture for pathway C and the crossover temperature is increased to 327 K, suggesting the stability of the ketimide catalyst at 100 °C toward intramolecular C−H activation. When $\Delta S^{\ddagger}_d = -8.5$ cal/(mol K) (experimental value for ketimide), the catalyst is still stable at 100 °C toward C−H activation via pathway C. However, it must be kept in mind that this reaction would occur at 250 °C.

The most interesting result is the lowest crossover temperature estimated for the constrained-geometry catalyst involving fluoride transfer to the cationic metal center. This reaction would occur below room temperature at all three different activation entropies.

The crossover temperatures for bis(phosphinimide) systems are 388, 422, and 522 K, corresponding to activation entropies $\Delta S^{\ddagger}_d = 0$, −2.7, and −8.5 cal/mol K, respectively. The bis(phopshinimide) catalyst system does not decompose at 100 °C via fluoride transfer to the metal center. If $\Delta S^{\ddagger}_d = -8.5$ cal/mol K, the bis-(phosphinimide) catalyst may also be active at 250 °C. The crossover temperatures for the other decomposition pathways depicted in Schemes 3−6 are high, and thus, these deactivation pathways would not occur at 100 and 250 °C.

Conclusions

In summary, we have presented a combined density functional theory and molecular mechanics investigation of deactivation pathways involving ion pair systems used as catalysts in olefin polymerization. Indeed, the present work on ion pair deactivation pathways may be regarded as a culmination of our previous theoretical work on aryl group transfer to the metal center[12] and hydride transfer to the growing polymer,[13] as well as decomposition involving the bare cation.[22] The transfer

Scheme 6. Aryl Group Transfer to the Metal Center and $CH_3B(C_6F_5)_2$ Transfer to Nitrogen of the Ancillary Ligand

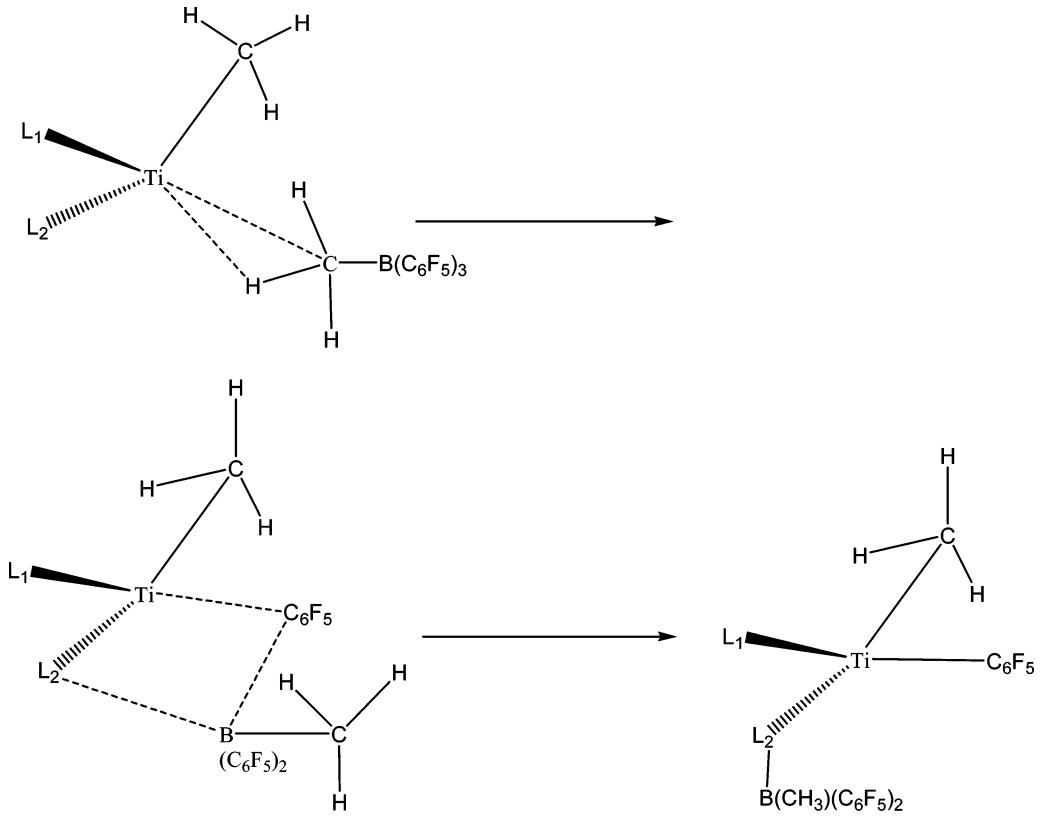

TS

Table 6. Crossover Temperatures (K) for Different Decomposition Pathways

decomposition pathway		crossover temperature		
Scheme 1	(pathway A)	797[a]	868[b]	1074[c]
	(pathway B)	667	726	726
	(pathway C)	300	327	404
Scheme 2	(CGC)	106	116	143
	(bis-phosphinimide)	388	422	522
Scheme 3	(CGC)	724	789	976
	(bis-phosphinimide	803	875	1082
Scheme 4	(CGC)	1527	1664	2130
	(bis-phosphinimide)	1718	1871	2314

[a] $\Delta S^{\ddagger}_d = 0.0$ cal/mol K. [b] $\Delta S^{\ddagger}_d = -2.7$ cal/mol K. [c] $\Delta S^{\ddagger}_d = -8.5$ cal/mol K.

of an aryl group from the counterion to the growing polymer and the transfer of fluoride from the counterion to the metal center are likely decomposition pathways.

The transfer of fluoride from the counterion to the metal center is the most facile decomposition pathway we have considered so far. However, the transfer of $B(C_6F_5)_3$ to the ancillary ligand (N) and transfer of aryl from $[MeB(C_6F_5)_3]^-$ to the metal center and $CH_3B(C_6F_5)_2$ to the ancillary ligand and the exchange of methyl on butyl with an aryl group in $B(C_6F_5)$ are not likely decomposition pathways for the catalysts considered in this investigation.

We have also studied three potential deactivation pathways that involve hydrogen transfer reactions. The transfer of hydrogen from the counterion to the growing polymer is the most likely decomposition pathway.

The various decomposition pathways considered in this study can be prevented if we employ bulky substituents on the ancillary ligands. For example, the sterically open systems deactivate much faster than systems that involve sterically demanding substituents. Also, the decomposition pathways can be eliminated if we employ electron-donating substituents on the ancillary ligands.

Acknowledgment. This work was supported by the Natural Science and Engineering Research Council of Canada (NSERC) and by NOVA Research and Technology Corporation (NRTC). T.Z. would like to thank the Canadian government for a Canada Research Chair.

Supporting Information Available: This material is available free of charge via the Internet at http://pubs.acs.org.

OM049157G